THE SELECTIVITY OF UV-LIGHT ACTIVATED METAL OXIDE SEMICONDUCTOR GAS SENSORS MANIFESTED BY TWO COMPETING REDOX PROCESSES

BY

WENTING LI, B. ENG.

A Thesis
Submitted to the school of Graduate Studies
In Partial Fulfillment of the Requirements
For the Degree
Master of Applied Science

McMaster University

MASTER OF APPLIED SCIENCE (2015) MCMASTER UNIVERSITY
(Materials Science& Engineering) Hamilton, Ontario

TITLE: The selectivity of UV-light activated metal oxide semiconductor gas sensors manifested by two competing redox processes

AUTHOR: Wenting Li, B. ENG. (Tianjin University, China)

SUPERVISOR: Dr. Gu Xu

NUMBER OF PAGES: 54

Abstract

The selectivity mechanism of the UV-light activated metal oxide semiconductor (MOS) gas sensors was studied. A reaction model based on two competing redox processes was presented to solve the selectivity problem. A concept named dynamic equilibrium of adsorbed oxygen concentration was brought about in this model and two reaction responses were discussed: (1) when most of the MOS surface is adsorbed with oxygen, the resistance of the MOS gas sensor will decrease upon the injection of reducing agents (RAs); (2) when most of the MOS surface is not adsorbed with oxygen, the resistance of the MOS gas sensor will decrease upon the injection of RAs. Finally, experiments were conducted on ZnO MOS gas sensors to prove the proposed hypothesis of the reaction mechanism.

Acknowledgement

I am deeply grateful to my supervisor, Prof. Gu Xu, for patient guidance and unwavering encouragement. Thank you so much for offering me such a valuable research opportunity. I’ve learned a lot from you during this journey and become a better self.

I would also like to thank my colleagues and all the friends who supported me during my graduate studies. I thank Dr. Cindy X. Zhao, Lucy L. Deng, Sean S. Chen, Alice Y. Mao and Olivia Y. Zhao for their inspiring suggestions and invaluable friendship.

I really appreciate the help from all the professors who have instructed me on the research and courses. And also, I want to give my thankfulness to all the technicians and staff members in MSE department.

Last but not least, I would like to thank my parents and grandparents in China, for supporting me, encouraging me and trusting in me. Thank you so much and I miss you a lot.

Table of Contents

Abstract iii

Acknowledgement iv

List of Figures vii

List of Tables x

Chapter 1 Introduction 1

- 1.1 Gas sensors and their applications 1
- 1.2 Typical types of gas sensors 2
  - 1.2.1 Electrochemical sensors 3
  - 1.2.2 Catalytic sensors 5
  - 1.2.3 Infrared sensors or IR detectors 7
  - 1.2.4 Metal Oxide Semiconductor sensors 10
  - 1.2.5 Comparison between different sensor techniquese 13
- 1.3 Two types of MOS gas sensors 15
  - 1.3.1 Heat activated MOS gas sensors 15
  - 1.3.2 UV light activated MOS gas sensors 16
- 1.4 Current challenges for UV-light activated gas sensors 17
- 1.5 Thesis overview 18

Chapter 2 Literature Review 20

- 2.1 Important parameters for UV-light activated MOS gas sensors 20
  - 2.1.1 Photoconductivity 20

2.1.2 Gas Sensitivity 21
2.1.3 Selectivity 21
2.1.4 Response and recovery time 21
2.1.5 Reversibility 22
2.1.6 Long-term stability 22
2.2 Operation mechanism of UV-light activated MOS gas sensors 23
2.2.1 The band theory 23
2.2.2 Material choice 24
2.2.3 Conduction models 25
2.3 Remaining challenges 32
2.3.1 Selectivity problem 32
2.3.2 Two conflicting reaction mechanisms 34
Chapter 3 Our New Hypothesis and Verification 37
3.1 Solving the conflict between the two redox processes 37
3.2 Solving the selectivity problem 39
3.3 Experimental verification 41
Chapter 4 Experimental Procedures 43
4.1 Sensor material, substrate and fabrication 43
4.2 Sensor testing 44
Chapter 4 Conclusion 46
Bibliography 47

List of Figures

Figure 1.1 Electrochemical sensors 3

Figure 1.2 Typical electrochemical sensor setup 4

Figure 1.3 A catalytic bead sensor (a); detector schematic diagram (b); catalytic sensor operating circuit (c) 6

Figure 1.4 Absorption bands of common gases between 2.5 and 5 μm; absorption bands of common gases between 6 and 12 μm 9

Figure 1.5 Infrared detector measuring scheme 9

Figure 1.6 Metal oxide thin film utilized as chemoresistive detector for gas chromatography 10

Figure 1.7 (a) Sintered-block gas sensor and (b) planar-film gas sensor with interdigitated electrodes 11

Figure 1.8 Schematic of a heat-activated sensor: thick films were deposited onto substrates 16

Figure 1.9 Scheme of the UV-light activated MOS gas sensor 17

Figure 2.1 Schematic band diagrams of an insulator, semiconductor and conductor 24

Figure 2.2 Schematic diagram of the gas sensing mechanism 27

Figure 2.3 Schematic diagram of band bending after chemisorption of charged species; EC, EV and EF represents conduction band, valence band and Fermi level, respectively; Δair denotes the thickness of the electron-depleted layer;

eVsurface represents the potential barrier 28

Figure 2.4 Structural and band models of conductive mechanism upon exposure to reducing agents. (a) with or (b) without CO 29

Figure 2.5 Schematic model of MOS grain size and the conducting mechanism. (a) The grain size is larger than twice the Debye length; (b) the grain size is smaller than twice the Debye length 30

Figure 2.6 Schematic gas sensor response transient 31

Figure 2.7 Plot of sensitivity vs. light intensity when nanoparticulate ZnO sensors were exposed to four RAs 32

Figure 2.8 Variation of resistance with temperature at different radiation flux density 33

Figure 2.9 (a) Light intensity vs. sensitivity for 100 and 300 ppm of ethanol; (b) current responses of the ZnO fiber sensor to ethanol gas with different ethanol concentrations 35

Figure 3.1 (a) Schematic illustration of the current response of a MOS sensor to UV irradiation. (b) Schematic illustration of the adsorbed oxygen species on a sensor surface. 37

Figure 3.2 Schematic representation of the influences of UV light intensity and the analyte reducing ability under UV light on adsorbed oxygen species concentration 40

Figure 3.3**.** Current responses of the ZnO film sensor to acetone vapor under UV irradiation: (a) Current response before annealing. (b) Current response after annealing under 350°C for two hours. (c) Current response of the annealed sample after 24 hours of UV light treatment 42

Figure 4.1 Schematic diagram of the sensor testing system 44

List of Tables

Table 1.1 Some common diseases identified by volatile organic compounds 2

Table 2.1 Sign of resistance change to change in gas atmosphere 26

Chapter 1 Introduction

1.1 Gas sensors and their applications

The sensorial perception of the surroundings is very important for the development of animal and human lives. Humans will respond differently to various smells like sour meat and rotten eggs to avoid the danger of intaking unhealthy foods. Nevertheless, the human olfactory system can only detect a few kinds of gases qualitatively. [1] Thus, the detection of poisonous CO, explosive liquefied petroleum gas and other dangerous vapors will acquire the assist of modern sensor technology. And the ethanol sensors can take the place of traditional detection methods for finding out drunken drivers.[1] Furthermore, some intrinsic correlations between breathe odors and diseases can be utilized in medical diagnostics. In 1971, Pauling et al[2] separated and quantitated 250 substances in human breath by gas-chromatograph method. The research of the relationship between human breath and disease diagnostics has attracted the research community since then.[3-6] Some organic compounds for the identification of several common diseases are shown in **Table**

1.1. Although the reliability of this kind of method is still under investigation, the advantageous of non-invasive and convenient compared with traditional detecting approaches make gas sensors very promising.

Table 1.1 Some common diseases identified by volatile organic compounds

Disease	**Compound(s)**
Asthma	Leukotrienes[7]
Liver disease	Hydrogen disulfide, limonene[8]
Non cholestatic	Hydrogen disulfide, 2-propanol[8]
Breast cancer	Quinazolinone, 1-phenyl-ethanone, Heptanal[9]
Sleep apnea	Interleukin IL-6, 8-isoprostane[10]
Uremia/kidney failure	Dim ethylamine, trim ethylamine[11]
Diabetes	Acetone[12]

1.2 Typical types of gas sensors

Gas sensors can be classified according to the operation mechanism (semiconductors, oxidation, catalytic, infrared, etc.).[13] The four typical ones are electrochemical sensors, catalytic sensors, infrared sensors or IR detectors and metal oxide semiconductor sensors.

1.2.1 Electrochemical sensors

The working principle of electrochemical gas sensors is that the target gas was oxidized or reduced at an electrode and the gas concentration was measured through the resulting current.[14] The oldest electrochemical sensors date back to the 1950s and were used for oxygen monitoring.[15] By the mid-1980s, miniaturized electrochemical sensors were utilized in the detection of toxic gases, with the sensor exhibiting good sensitivity and selectivity.[15] **Figure** 1.1 shows some electrochemical sensors.

Figure 1.1 Electrochemical sensors[16]

A typical electrochemical sensor consists of a sensing electrode (or working electrode), and a counter electrode separated by a thin layer of electrolyte, **Figure** 1.2.

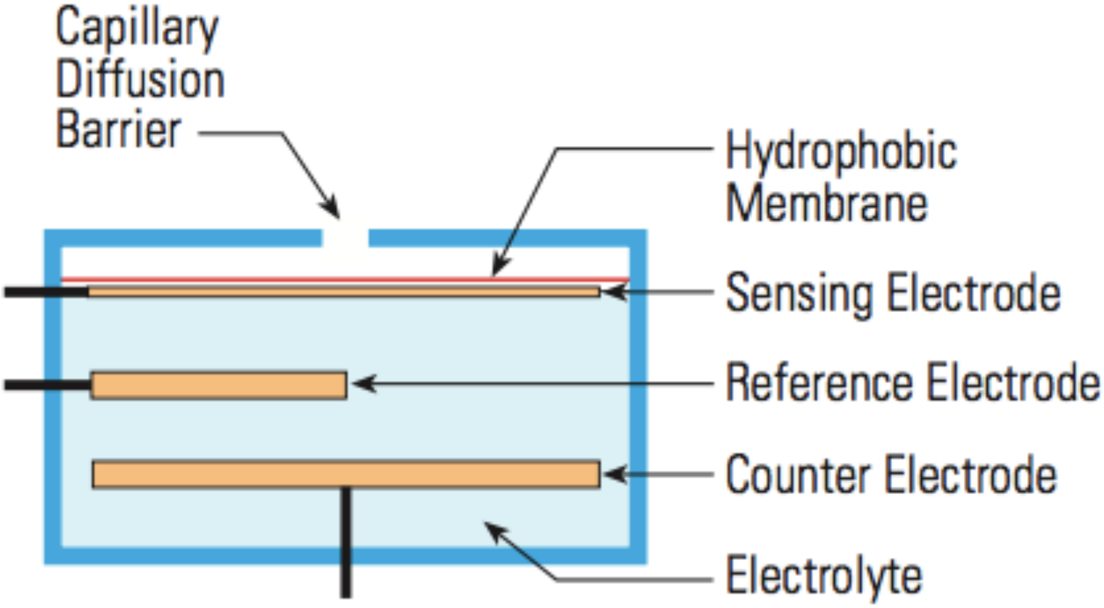

Figure 1.2 Typical electrochemical sensor setup[15]

The gas first passes through a capillary diffusion opening and then diffuses through a hydrophobic barrier, and then gets in contact with the electrode surface.[15] The hydrophobic membrane can allow the gas to pass through to get in touch with the sensing electrode while at the same time prevent the electrolyte to get out. The gas that gets to the other side of the membrane reacts on the sensing electrode. An oxidation or reduction reaction is catalyzed by the electrode material specifically developed for the gas of interest. A current proportional to the gas concentration flows between the anode and the cathode and can be used to determine the gas concentration. Typical reactions are shown in equations below.

$$\text{Anode: } CO + H_2 \rightarrow CO_2 + 2H^+ + 2e^- \quad [15]$$

$$\text{Cathode: } O_2 + 4H^+ + 4e^- \rightarrow 2H_2O \quad [15]$$

It is very important to have a stable and constant potential at the sensing electrode. In reality, the sensing electrode potential does not remain constant due to the continuous electrochemical reaction taking place on the surface of the electrode. To improve the performance of the sensor, a reference electrode is introduced. A fixed stable potential is applied to the sensing electrode. The reference electrode maintains the value of this fixed voltage.[15]

1.2.2 Catalytic sensors

A catalytic sensor is a type of sensor that is used for combustible gas detection known as pellistors.[17] It is often called as catalytic bead sensors for their shape, which is shown in **Figure** 1.3(a). Catalytic-type gas sensor consists of two elements: a detector element (D) that contains catalytic material and is sensitive to combustible gases, and a compensator element (C) that is inert.[18] A schematic detector diagram is shown in **Figure** 1.3(b).[19] The detector consists of a very fine coil of platinum wire, embedded with a ceramic pellet.[19] On the surface of the pellet is a layer of a high surface area noble metal,

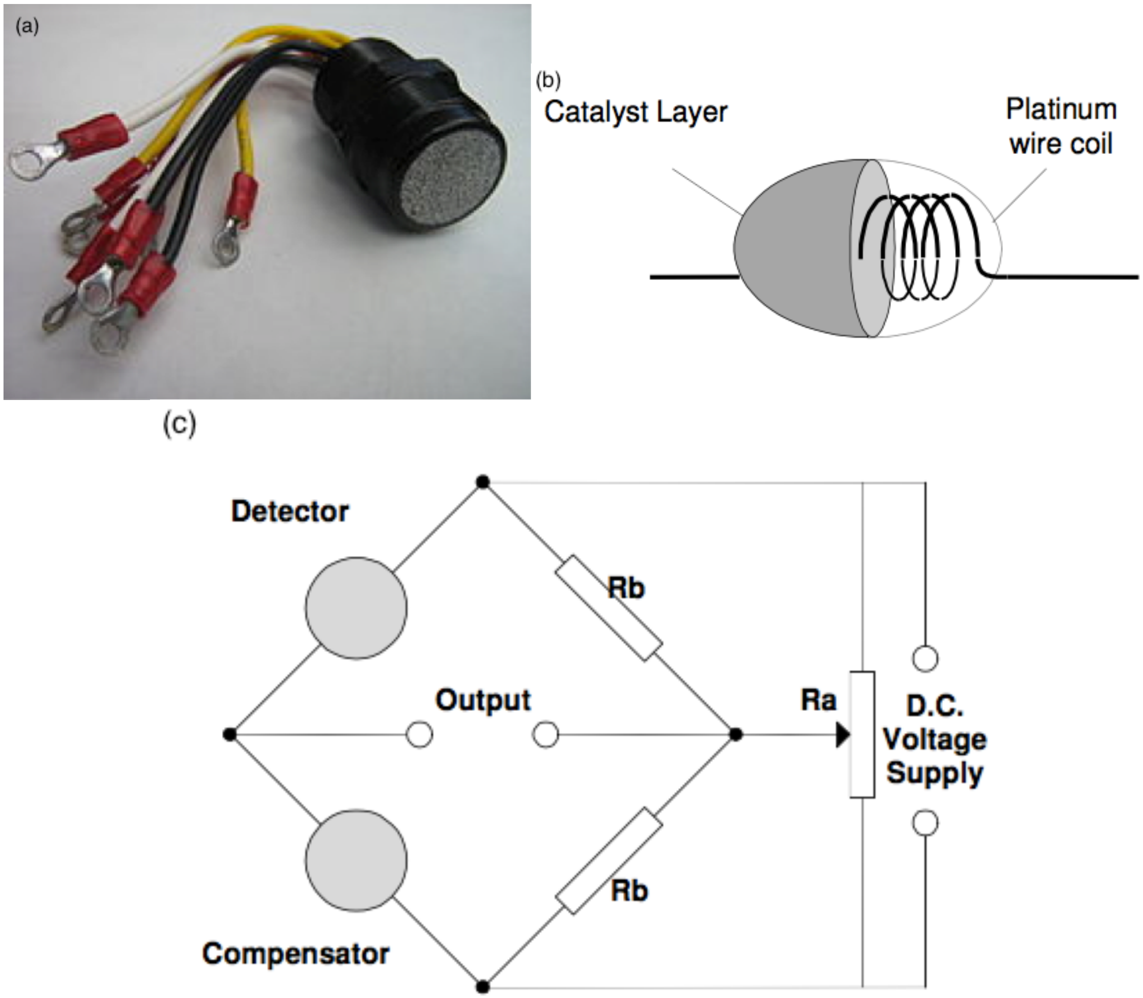

Figure 1.3 A catalytic bead sensor (a)[17]; detector schematic diagram (b)[19]; catalytic sensor operating circuit (c)[19]

which, when hot, acts as a catalyst to promote exothermic oxidation of flammable gases.[19] Combustible gases will burn only on the detector element, causing a rise in its temperature and, as a result, a rise in its resistance.[18] The compensator's temperature and resistance will remain unchanged in the presence of combustible gases.[18] Normally the detector and the compensator will form a Wheatstone bridge circuit, which is shown in **Figure** 1.3(c). The change of the resistance of the detector under the influence of combustible gases will cause an imbalance in the bridge circuit, thus producing an output voltage.[19] The output voltage signal is proportional to the concentration of combustible gases.[18] Gas concentration can be determined by measuring the output voltage.

1.2.3 Infrared sensors or IR detectors

In 1800, the astronomer Sir William Herschel demonstrated the existence of a considerable amount of energy in the solar spectrum beyond the red end of the visible spectrum, what we now term infrared (IR) radiation.[20] Since then many scientists have devoted their efforts to IR gas sensing. But it was not until the development of non-dispersive infrared (NDIR) techniques that practical IR gas sensors were possible.[20] Infrared gas sensors work based on the principle of infrared absorption.[21] Gases whose molecules consist of two or more dissimilar atoms absorb infrared radiation in a unique manner and are detectable using infrared techniques.[22] The infrared spectrum between 2 and $20\mu m$ is of use in gas detection because it is here that many gases show characteristic vibration/rotation absorption spectra with narrow, non-overlapping bands[23], **Figure** 1.4. A typical Infrared measurement system is shown in **Figure** 1.5. An infrared source illuminated a volume of gas that has entered inside the measurement chamber.[21] The gas absorbs some of the infrared wavelengths as the light passes through it, while others pass through it completely unattenuated.[21] The amount of absorption is related to the concentration of the gas and is measured by a set of optical detectors and suitable electronic systems.[21] Because factors other than gas can lead to a change in the detected

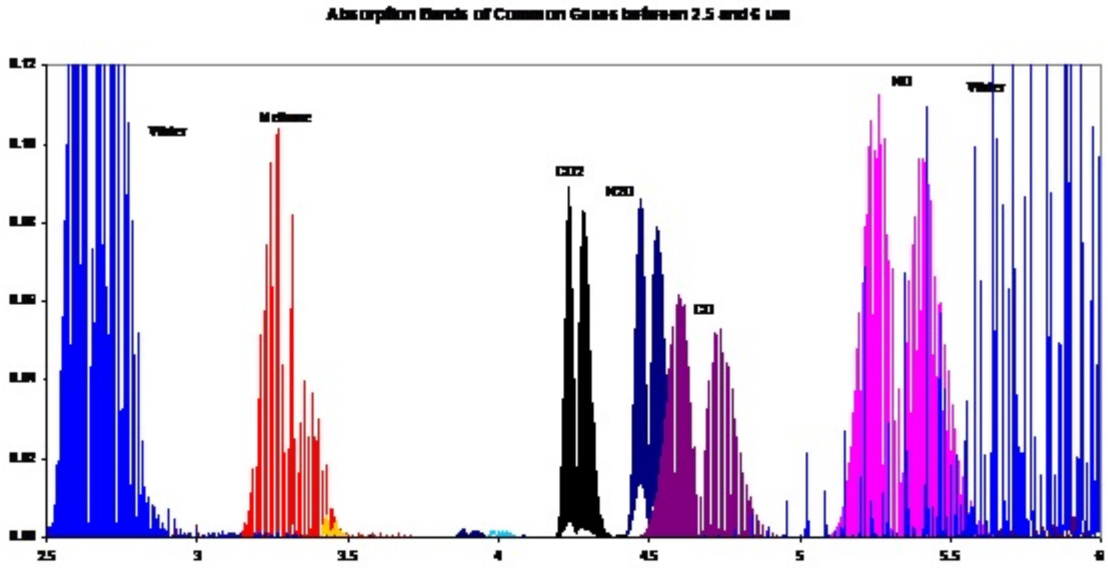

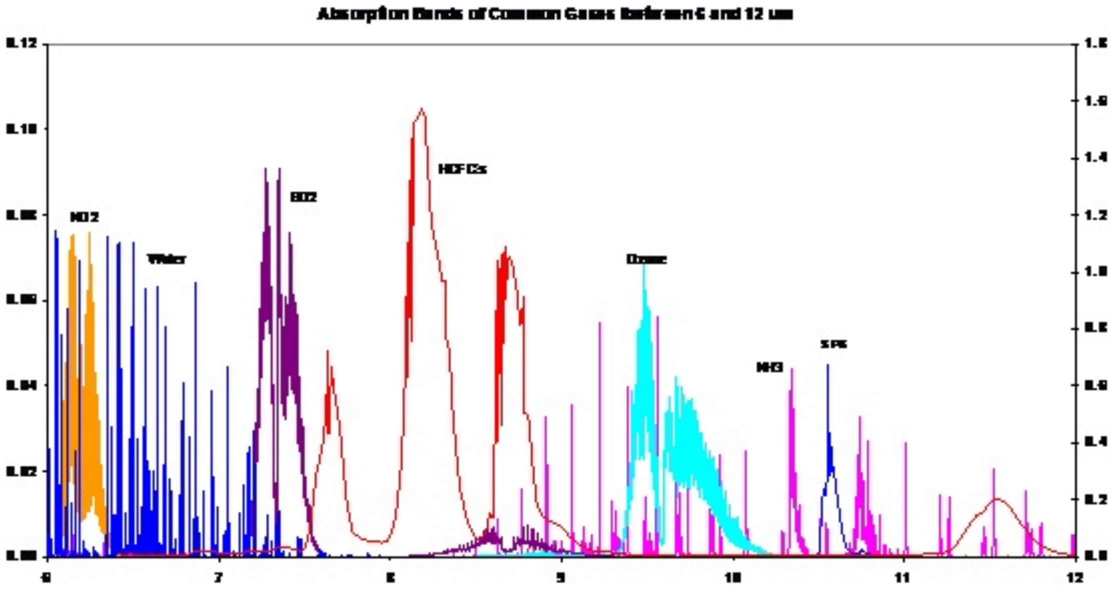

Figure 1.4 Absorption bands of common gases between 2.5 and 5 μm; absorption bands of common gases between 6 and 12 μm[23]

signal, causing a reading error.[24] A reference signal detector is introduced into the system. It is equally affected by all the non-gas phenomena, so by taking the ratio of the signals from the two detectors we can eliminate or reduce the effect of other factors.[24]

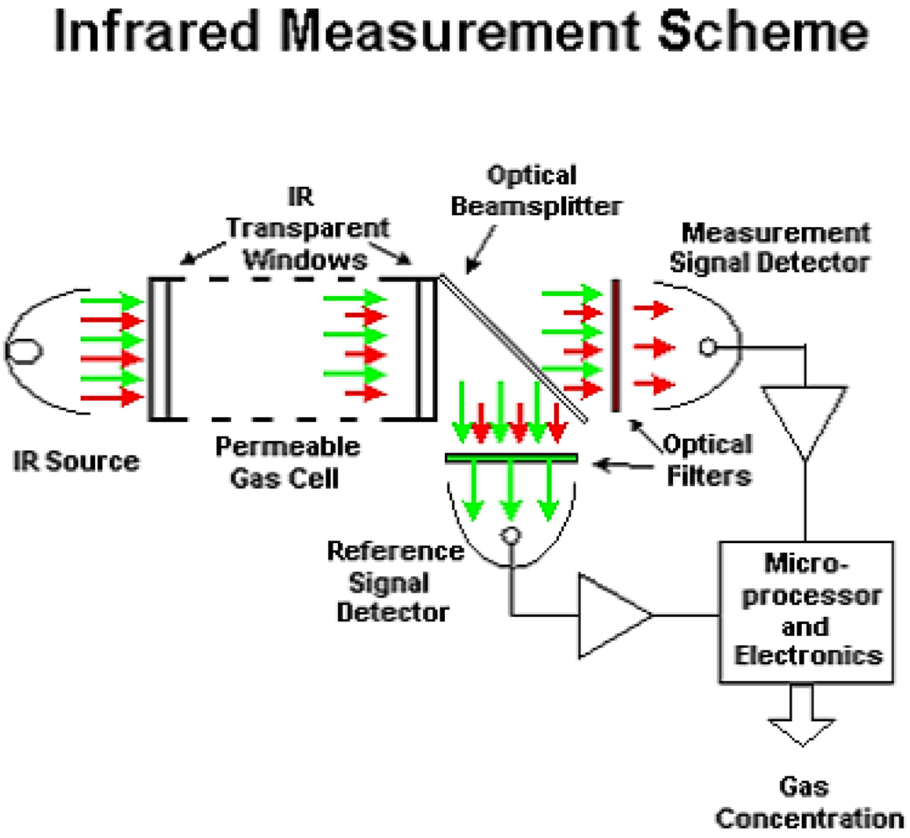

Figure 1.5 Infrared detector measuring scheme[21]

]

1.2.4 Metal Oxide Semiconductor sensors

Metal Oxide based gas sensors have been developed in the second half of the 20th century[1] after the absorption or desorption of a gas on the surface of a metal oxide changes the conductivity of the material was found out in 1962[25]. The advantages of low cost, simplicity of assembly[25], flexibility of usage and large number of detectable gases/possible application fields[26] make them a very desirable technology to exploit. The first application was using ZnO thin films as chromatographic detectors[1], **Figure** 1.6. Although the response time was not as ideal as traditional methods, the sensitivity was 100-times higher[1]. Since then, many efforts have been devoted to the metal oxide gas sensor market to improve their performances. The change in device structure, different synthesis methods, the adding of various additives and other techniques have all been

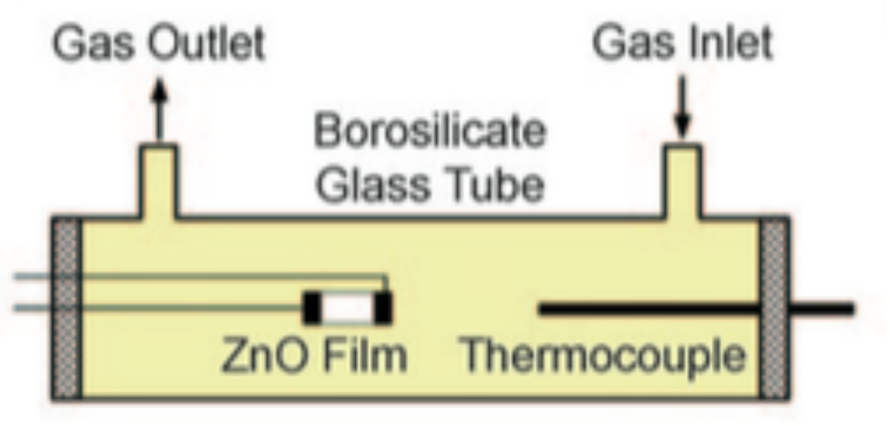

Figure 1.6 Metal oxide thin film utilized as chemoresistive detector for gas chromatography[1] tried by scientists all over the world. Different types of sensor substrates have been developed, eg. cylindrical and planar layouts[1], **Figure** 1.7, to help incorporating solid-state semiconductor sensors into micro-sized devices.[1]

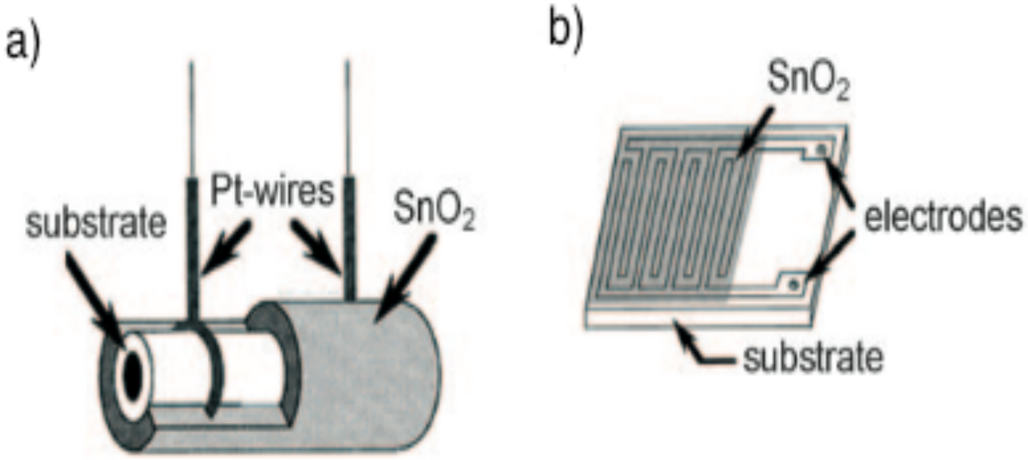

Figure 1.7 (a) Sintered-block gas sensor and (b) planar-film gas sensor with interdigitated electrodes[1]

The sensing properties can be improved by decreasing the metal oxide material grain size to nanoscale[1], for there's a higher efficiency of conversion from chemical interactions to electrical signal[26]. Furthermore, some one-dimension metal oxides whose grain sizes are comparable to twice the Debye length[1, 26]have been studied recently to achieve a higher sensitivity. But if the grain size is way too small, the sensitivity may get lower for there are possibilities of agglomerating and losses of structural stability[26]. Other techniques through changing the morphology besides decreasing the grain size can also improve the sensitivity. For example, different crystallographic facets exposed on the surface[26] and varying surface to volume ratio[1] can make a difference on the performance of the gas sensors, too. The adding of noble metal particles on the sensor surface can help increasing the sensitivity mainly through the spillover effects[1]. These particles work as high-effective oxidation catalysts[26] to enhance the reactions that are taken place on the sensor surface. Scientists also found that the composites of different metal oxides exhibit higher sensitivity than sensors constructed solely from one oxide.[26] Typical synthesis methods are chemical vapour deposition (CVD), screen-printing of ceramic powders, sol-gel techniques and physical vapour deposition (PVD).[25]

The basic working principle of metal oxide semiconductor (MOS) sensors is that the donor electrons in MOS are attracted by the oxygen species adsorbed on the sensor surface.[28] Then the introduced target gas reacts with these adsorbed species and the electrons will be released back to the conduction band of MOS and an electronic variation will take place[27]. By measuring the resistance change through the varying of capacitance, work function, optical characteristics and other parameters, the type and concentration of the target can be determined.[27] But not all of the MOS materials can be utilized in the sensing field. The transition-metal oxides (CuO, *etc*) are seldom chosen as sensor materials for they only have one oxidation state and more energy is needed to activate the reaction[27]. Actually, metal oxides with d^0 and d^{10} electronic configurations can be used in gas sensing applications.[26]

1.2.5 Comparison between different sensor techniquese

Electrochemical sensor technology has the advantages of:

- can be specific to a particular gas or vapour in the parts-per-million range[29];
- Linear output, low power requirements and good resolution[29];
- Excellent repeatability and accuracy[29];

They have the disadvantages of:

- Narrow or limited temperature range[29];
- Cross-sensitivity of other gases[29];
- Can not detect combustible gases[29];
- Relatively complicated system, involving three electrodes and electrolyte.

Catalytic sensors have the advantages of:

- Easy to install, calibrate and use[30];
- Long lived with a low life-cycle cost[30];
- Immensely flexible with application[30];

They have the disadvantages of:

- Catalysts can be poisoned due to contamination[30];
- Prolonged exposure to high concentrations of combustible gas will lead to degradation of sensor performance[30].

IR detectors have the advantages of:

- No contamination or poisoning problems[30];
- No routine calibration[30];

- Oxygen not needed for operation[30];
- Not easily influenced by ambient atmosphere.

Their disadvantages are:

- Higher cost;
- Gases must be infrared active;
- Lower ambient temperature[30].

Advantages of MOS gas sensors:

- High sensitivity[31];
- Good stability[31];
- Long life time[31;
- Low cost[31];

Their disadvantages:

- Easily interfered by other gases[31];
- Relatively longer recovery time[31];
- Oxygen concentration, humidity and temperature have large influence on sensor performance[31].

In this study, we choose MOS gas sensors to conduct the research. Because their characteristics of low cost, portable, high sensitivity and easy to fabricate make MOS sensors very promising products for various applications.

1.3 Two types of MOS gas sensors

The operation of MOS gas sensors needs some external factors to trigger. The most common ones are activated by heat and activated by UV light.

1.3.1 Heat activated MOS gas sensors

The surface redox reactions need large activation energy, thereby a high operating temperature is needed for the MOS sensor to work.[32] Thus, a heater must be incorporated into the sensor device. An example is shown in **Figure** 1.8. In air, the electrons in the oxides are attracted by the oxygen species adsorbed on the sensor surface, impeding the flow of current.[28] Under room temperature, the ionized oxygen is only chemisorbed onto the surface in its molecular form, O_2^-, which is less reactive.[36] At higher temperatures, the O_2^- can be dissociated into more active species as O^- and O^{2-}[36] to promote the reactions between these oxygen species and target gases.

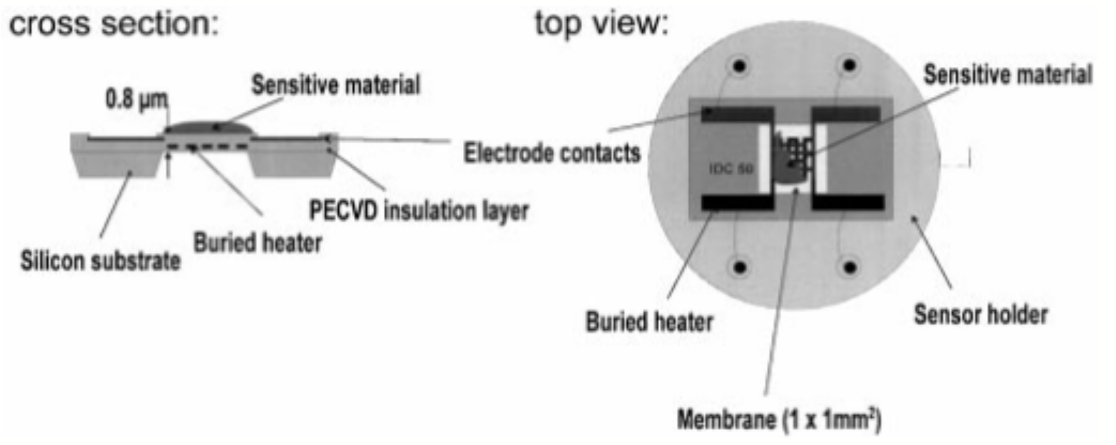

Figure 1.8 Schematic of a heat-activated sensor: thick films were deposited onto substrates[44]

1.3.2 UV light activated MOS gas sensors

Although nowadays, most of the MOS gas sensors are heat activated ones. But they cannot detect flammable, explosive gases and biospecies. To overcome this limit, Saura[34] developed the UV activated SnO_2 films to detect trichloroethylene and acetone vapor at room temperature, which has been follow by many other research groups to investigate in this field. A typical UV-light activated MOS gas sensor device in shown in **Figure** 1.9. The sensor usually works inside a sealed chamber with a gas-inlet hole and a gas-outlet hole to make sure there is a gas flow. The light source is chosen under the condition that the energy provided can trigger the reaction inside the metal oxides. Because this is our main research interest here, the detailed reaction mechanisms will be discussed in Chapter 2.

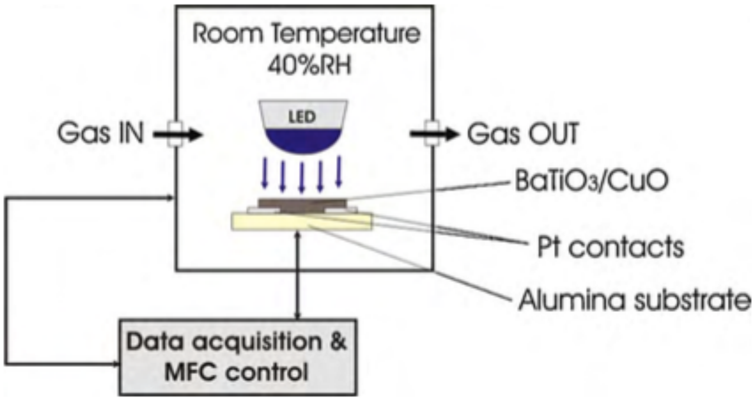

Figure 1.9 Scheme of the UV-light activated MOS gas sensor[33]

1.4 Current challenges for UV-light activated gas sensors

Although many scientists have devoted their efforts to UV-light activated MOS gas sensors research, the fundamental reaction mechanism is still not very clear. Some scientists found that by changing the intensity of the UV light, a maximum sensitivity can be found for each analyte in a different location under different intensity values, indicating that it is possible to achieve the selectivity of the MOS sensors by varying the UV-light intensity. Several theoretic models[37-39] were proposed to discuss the detection mechanisms that are involved in the selection process. But no satisfactory results have been found so far. The variation in intensity will not affect the energy states in the MOS gas sensor. Therefore a better theory needs to be developed to provide the rationale of the selectivity here.

Moreover, two conflicting reaction mechanisms have been found in the previous studies. Jian et al.[40,41] claimed that the reducing agents (RAs) consume charge carriers thus decrease the conductivity of the sensing materials. But other groups[36,42,43] found that upon injection of RAs the electrons would be released back to the conduction band of the MOS, leading to the increase of the conductivity of the sensing materials. Therefore, the new theory should also be able to resolve this conflict, which has to be further verified by experimental results.

1.5 Thesis overview

The thesis contains five chapters. *Chapter 1* made a brief introduction on the different types of gas sensors, including electrochemical sensors, catalytic sensors, Infrared sensors and MOS sensors. The advantages and disadvantages of these four kinds were also discussed. And then two types of MOS gas sensors were introduced. It is followed by the detailed literature reviews in *Chapter 2*. An overview was given on the working principles and operating parameters of UV-light activated gas sensors. The remaining challenges are also discussed in this chapter. In *Chapter 3*, a new hypothesis is brought about to resolve the problems mentioned in *Chapter 2*. *Chapter 4*, experimental procedures, includes the details of device fabrication, gas sensing measurements to improve our hypothesis. Finally, the main conclusions of this study are summarized in *Chapter 5*.

Chapter 2 Literature Review

2.1 Important parameters for UV-light activated MOS gas sensors

2.1.1 Photoconductivity

The activation of MOS gas sensors needs super band light to trigger. It is found that a large current increase was observed on exposing the material to UV-light whose energy is larger than the bandgap.[35,40] The increase is typically three to four orders of magnitude.[35] The reason for this phenomena is that the electron-hole pairs are generated inside the MOS by the UV-light, thus the carrier density and intra-grain conductivity[35] are increased.

2.1.2 Gas Sensitivity

The sensitivity is often decided by two factors: 1) the minimum concentration of a target gas that can be detected by a gas sensor; 2) the response: it is usually defined as, $S_g = \frac{X_g - X_a}{X_a}$, where X_g is the tested response value in the target gas environment and X_a is the response value in air. The X can be current, resistance, impedance, etc.

2.1.3 Selectivity

Selectivity is one of the most important characteristics of the MOS sensors. It determines whether a sensor can respond selectively to a group of analytes or even specifically to a single analyte. It's not applicable if the sensor cannot tell the type of gas it is detecting. Several approaches have been developed to improve the selectivity for the MOS gas sensors, the most common strategies are sensor arrays and the use of temperature protocols.[48] A selectivity by tuning the UV-light intensity is found recently by some scientists. The purpose of this study is to find the reason for this selectivity.

2.1.4 Response and recovery time

The response time is defined as the time required for the X reaching 90% of the stable value after injection of the target gas. The recovery time is defined as the time needed for the X to return to 10% above the initial value in air after cutting off the gas injection. The less the time needed, the better the performance of the sensor. For sensors using UV-light to activate the reactions, the MOS can remember the illumination event for some time[47]. Although the disorder caused by radiation can gradually relax itself after turning off the light[47], it is better to introduce some external forces to help eliminating this memory effect.

2.1.5 Reversibility

A good sensor should provide a stable and consistent detection performance for each test. It is found by J. D. Prades et al[46] that the conductance of ZnO nanowires could not return to its initial value after illuminating by UV-light and a persistent photoconductivity (PPC) exists in these nanomaterials. This impedes a higher performance for the MOS gas sensors. But the PPC can readily be reverted by heating the final devices or passivating the sensor surface.[46]

2.1.6 Long-term stability

The gas sensors should provide stable output signal under repetitive exposure to UV-light and testing gas ambient for practical usage. It is required that a sensing device should exhibit stable and reproducible signal for the period of at least 2-3 years[49]. The pure MOS materials cannot achieve this. Therefore, several strategies like doping, coating, changing of the morphology[49] have been adopted by manufactures to achieve long-term stabilities for MOS gas sensors.

2.2 Operation mechanism of UV-light activated MOS gas sensors

2.2.1 The band theory

The electrons of an isolated atom occupy atomic orbitals.[52] And molecular orbitals are formed by several atomic orbitals when multiple atoms are brought together.[52] As more and more molecular orbitals are formed, their energy levels will be very close.[53] Eventually, these energy levels form bands of energy. A valence band and a conduction band exist within a lattice.[25] The energy difference between these two bands decides the type of the material.[25] Three main types of material in band theory are shown in **Figure** 2.1.

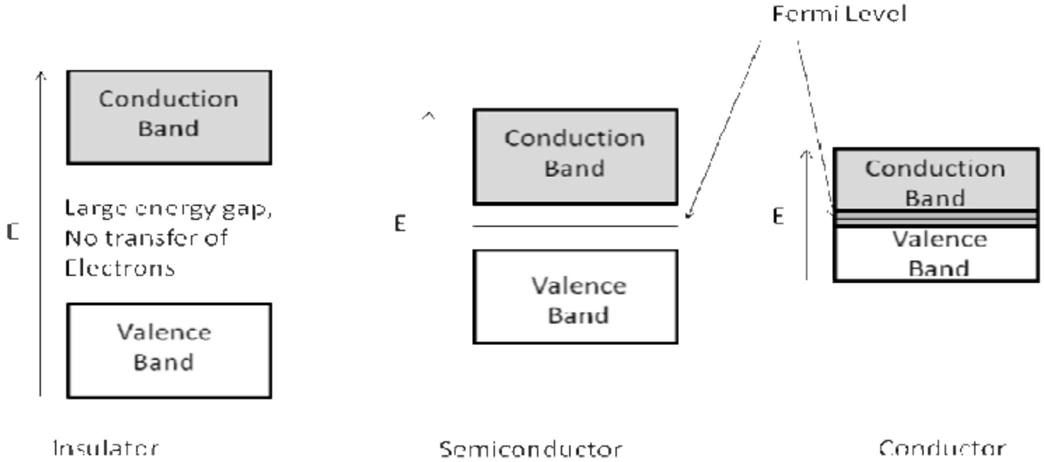

Figure 2.1 Schematic band diagrams of an insulator, semiconductor and conductor.[25]

The large energy gap between the two bands of an insulator, usually more than 5 eV[25], impedes the promotion of the electrons from the valence band to the conduction band. Thus, no conduction can occur. In conductors there is an overlap between the two bands.[54] Therefore, the electrons can flow easily resulting a high conductivity. The semiconductors, which are the materials being studied here, have a sufficiently large energy gap (0.5-5.0 eV)[25] so a certain external force is needed to help the promotion of electrons to the conduction band, such as heating, super-band UV-light exposure et al.

2.2.2 Material choice

Not all the semiconductors can be chosen as sensor materials. The semiconductors predominated by ionic bonds (ZnO, SiO_2, SnO_2) are better sensor materials than those covalent-bonded (Si, Ge, GaAs) for they have better sensing performances.[49] However, standard ionic semiconductors (ZnS, CdS) are poor in stability.[49] Thus, metal oxides become our best choices for they have relatively low native surface states concentration and high stability[49].

Metal oxides can be classified into two categories[49]:

- Transition-metal oxides (Fe_2O_3, NiO, Cr_2O_3, etc.) and
- Non-transition-metal oxides, which include (1) pre-transition-metal oxides (MgO, etc.) and (2) post-transition-metal oxides (SnO_2, etc).

Transitional metal oxides have d atomic orbitals, which results in variable oxidation states, are more preferred in surface chemistry modification than the $s-$ and $p-$symmetry in non-transition-metal oxides.[49] Too much energy is needed to add or remove electrons from the cations when non-transition-metal oxides are coordinated with O^{2-} ligands. However, the energy difference between a d^n and d^{n+1} or d^{n-1} configuration is rather small.[49] More precisely, transition-metal oxides with d^0 and d^{10} electronic configurations can be used in gas sensing applications.[27] The d^0 configuration is presented in transition metal oxides (TiO_2, V_2O_5, WO_3, etc) and d^{10} can be found in post-transition-metal oxides (SnO_2, etc).

2.2.3 Conduction models

Both n-type (ZnO, SnO_2, etc) and p-type (CuO, NiO_x, etc) metal oxides can be utilized as gas sensors. Electrons are the majority carriers in n-type metal oxides. The adsorbed oxygen species can attract these electrons and reduce conductance. The conductivity of n-type semiconductors is increased upon injection of reducing agents and decreased under oxidizing atmosphere, whereas a p-type semiconductor is a material that conducts with positive holes being the majority carriers. Therefore an opposite phenomena can be observed for them. A summary of the response is provided in **Table** 2.1[25].

Table 2.1 Sign of resistance change to change in gas atmosphere[25]

Classification	**Oxidizing Gases**	**Reducing Gases**
n-type	Resistance increase	Resistance decrease
p-type	Resistance decrease	Resistance increase

Because the most common application is testing reducing agents (RAs) using n-type MOS materials, here in this study we will use n-type material reacting with RAs as an example.

The basic working principle of UV-light activated gas sensors is shown in **Figure** 2.2.

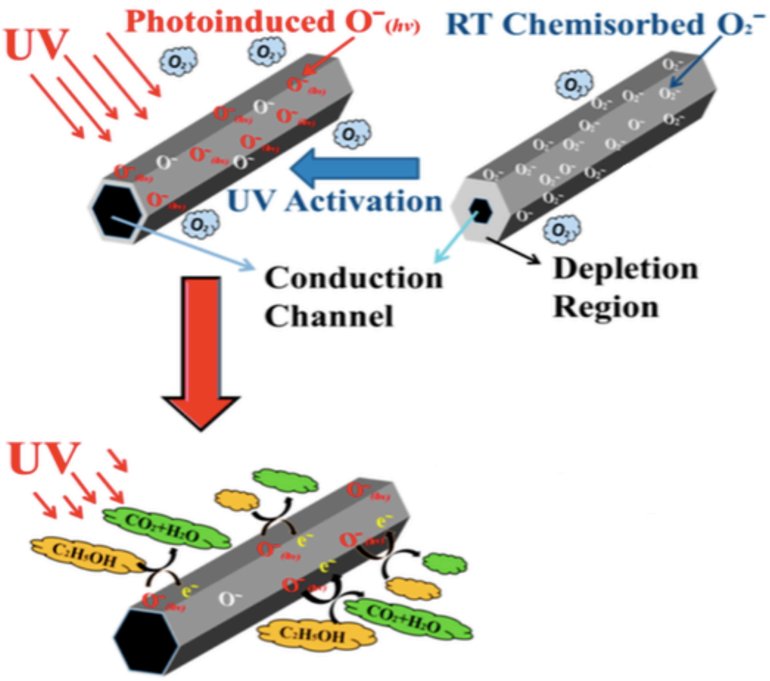

Figure 2.2 Schematic diagram of the gas sensing mechanism[36]

In the dark, the oxygen species in the atmosphere are adsorbed on the sensor surface and receiving electrons from the MOS. These trapped negative charge causes an upward band bending and an electron-depleted region[26] thus the resistance will get higher compared to the flat band situation, **Figure** 2.3.

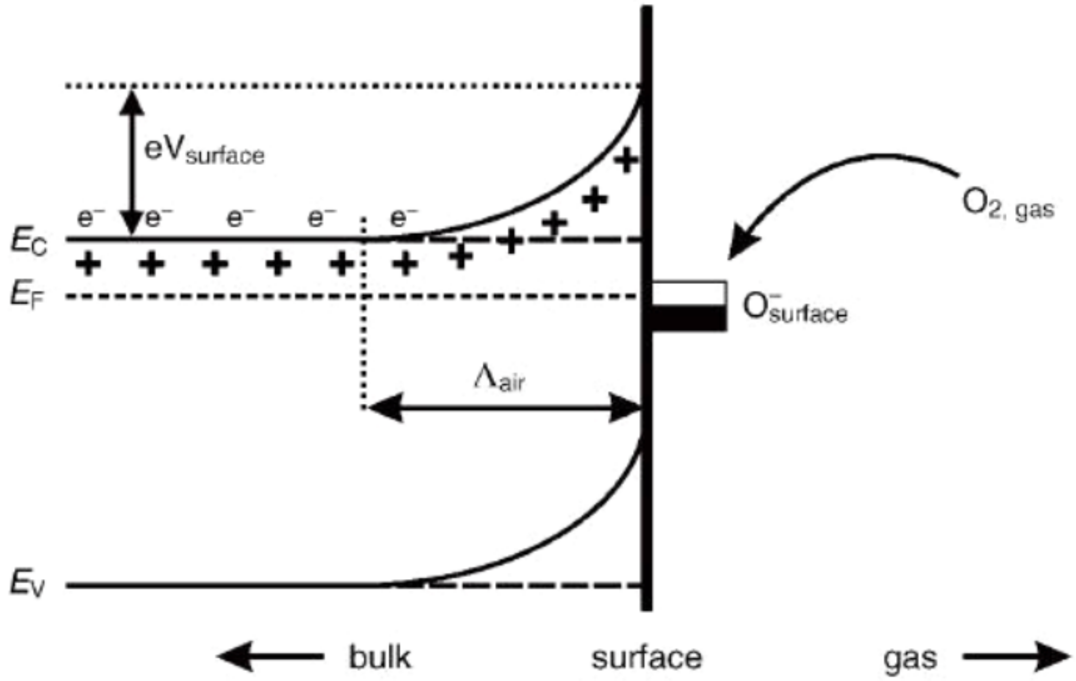

Figure 2.3 Schematic diagram of band bending after chemisorption of charged species; E_C, E_V and E_F represents conduction band, valence band and Fermi level, respectively; Δ_{air} denotes the thickness of the electron-depleted layer; $eV_{surface}$ represents the potential barrier.

When the sensor is shown by UV light that has higher energy than the band gap of the semiconductor material, the carrier density or the $e^- - h^+$ pairs will increase. And upon the creation of excition[36], the previously adsorbed O_2^- will become more active species as O^-/O^{2-}. Additional photoinduced oxygen ions are created because of the oxygen molecules reacting with the photoelectrons and creating $O_2^-(hv)$, which is weakly bonded to MOS and can be easily removed.[55] The holes in the material will migrate from bulk to surface and react with these adsorbed oxygen species.[55] So the electrons will be released back to the conduction band of the semiconductor. As a result, the resistance will decrease. When we introduce the reducing agents to the sensor surface, there will be two kinds of reactions that may take place:

1) The RA will react with the adsorbed oxygen species, and again release the electrons and the resistance will decrease. The band bending is reversed and electron-depleted region is narrowed.[26] Then the Schottky barrier between two grains is lowered[26, 55] and it would be easier for electrons to conduct through different grains for the mobility μ is higher[56, 57], **Figure** 2.4.

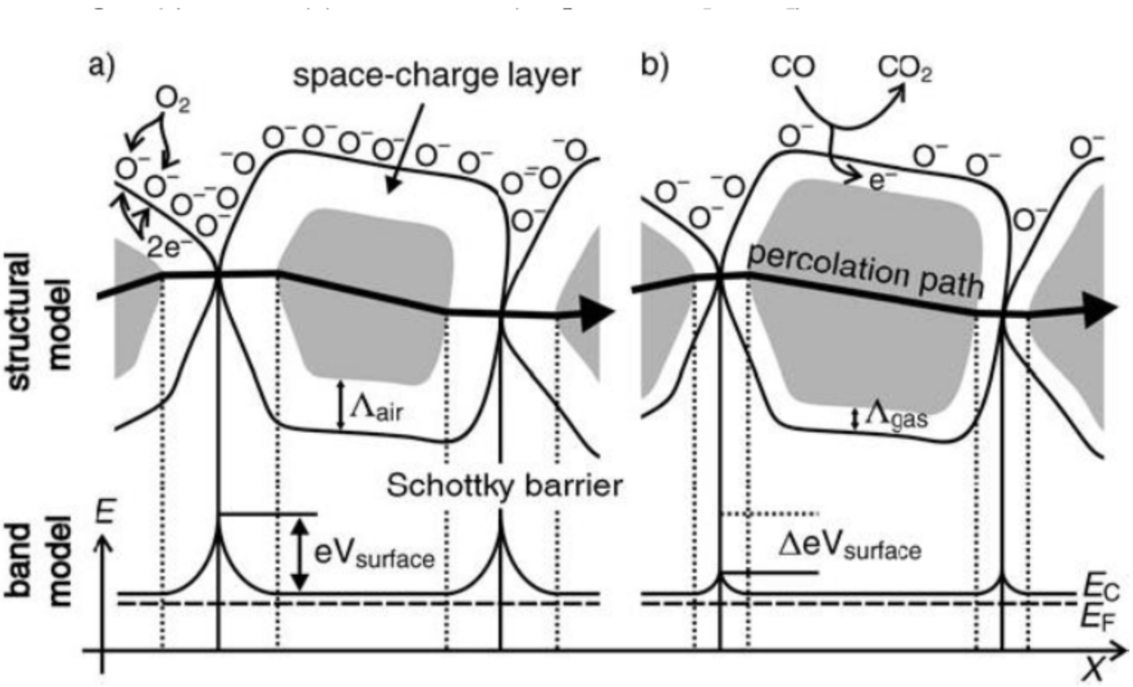

Figure 2.4 Structural and band models of conductive mechanism upon exposure to reducing agents. (a) with or (b) without CO[26]

But this is only suitable for MOS whose grain size is much larger than its Debye length. The mechanism is controlled by grain boundaries.[1] There are two other situations: when the grain size is barely larger than twice the Debye length, **Figure** 2.5 (a), a conduction channel exists within the grain, whose width L_c decides the conductivity. Therefore, this is controlled by neck. The third situation is shown in **Figure** 2.5 (b). The grain size is smaller than twice the Debye length, thus the grain is completely depleted. By reactions between the RAs and the adsorbed oxygen, a channel can be opened inside the grain and the mobility increases remarkably.

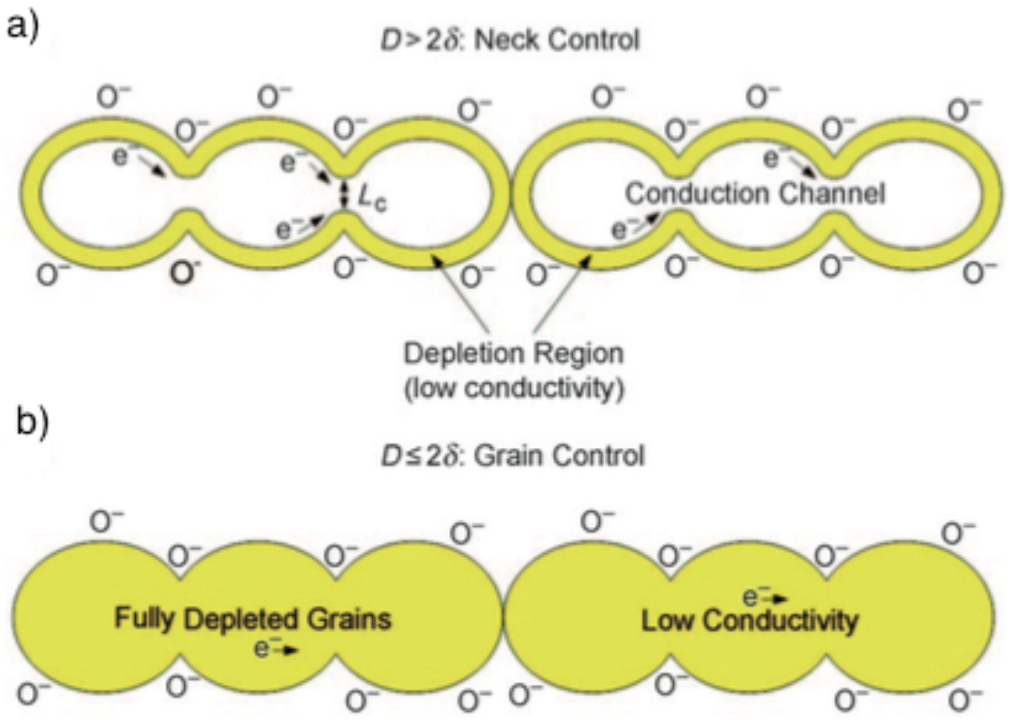

Figure 2.5 Schematic model of MOS grain size and the conducting mechanism. (a) The grain size is larger than twice the Debye length; (b) the grain size is smaller than twice the Debye length[1]

However, such small grains like in **Figure** 2.5 (a) and (b) have problems of sintering and low stability.[1] Hence the most common ones are MOS whose grain size is much larger than the Debye length.

2) The second one is that the RA will react directly with the MOS and the gas will consume both electrons and holes. Thus cause the carrier density to decrease and the resistance will increase.[40] The processes introduced above can be seen very clearly in **Figure** 2.6. By turning on the light, the resistance will decrease. And if RA reacts with MOS the resistance will climb up, however, if RA reacts with oxygen species, the resistance will continue to go down.

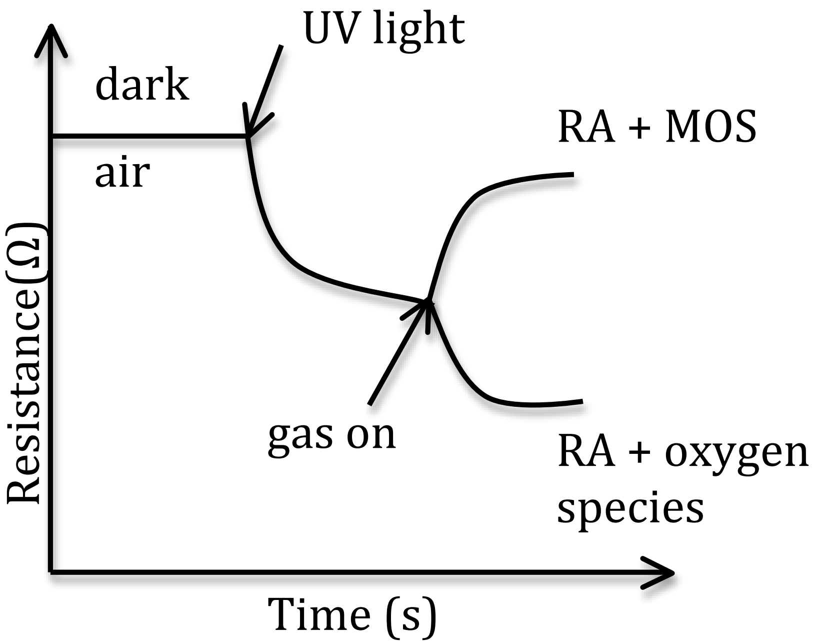

2.3 Remaining challenges

2.3.1 Selectivity problem

Selectivity is one of the most important characteristics of the MOS sensors. It’s not applicable if the sensor can’t tell the type of gas it’s detecting. De Lacy Costello et al[35], Alenezi et al[36] and Comini et al[47] found that by tuning the intensity of the UV light, a maximum sensitivity can be found for each analyte in a different location under different intensity values, **Figure** 2.7, indicating that it is possible to achieve the selectivity of the MOS sensors by varying the UV-light intensity.

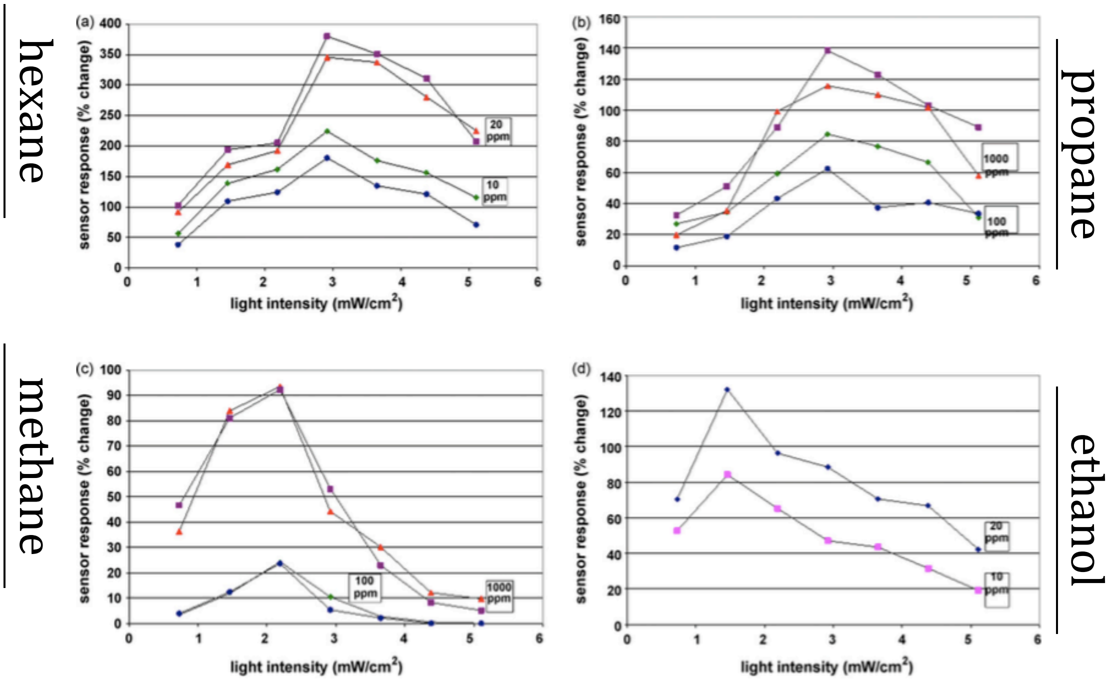

Figure 2.7 Plot of sensitivity vs. light intensity when nanoparticulate ZnO sensors were exposed to four RAs[35]

Several theoretic models[37-39] were proposed to discuss the detection mechanisms that are involved in the selection process. But no satisfactory results have been found so far. For example, a theoretical study, **Figure** 2.8, found that there should be an increased response with increased intensity.[37] But the experimental results say the different. So what's missing in the theoretical study?

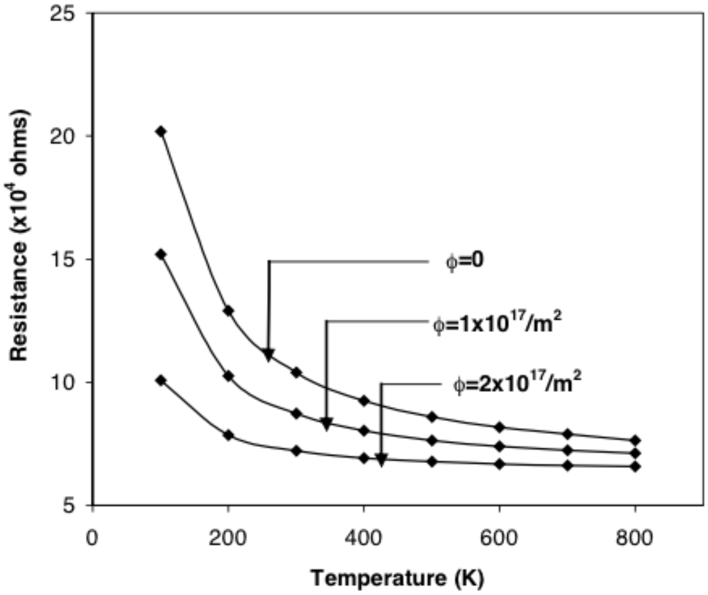

Figure 2.8 Variation of resistance with temperature at different radiation flux density[37]

Since the change in intensity only changes the number of photons emitted per second per unit area, and according to the Planck-Einstein relation $E = \frac{hc}{\lambda}$, where E is the energy of the emitted photon, h is the Planck constant, c is the speed of the light and λ is the wavelength of the photon, the energy of the photon does not change as long as the wavelength of the photon remains the same. Thus the variation in intensity will not affect the energy states in the MOS gas sensor. However, the amount of chemisorbed oxygen species, which plays a very important role in the sensing mechanism, will be changing under various intensities. Therefore a better theory needs to be developed to provide the rationale of the selectivity here.

2.3.2 Two conflicting reaction mechanisms

Moreover, two conflicting reaction mechanisms have been found in the previous studies. Jian et al.[40, 41] claimed that the reducing agents (RAs) consume charge carriers thus decrease the conductivity of the sensing materials. But other groups[36, 42, 43] found that upon injection of RAs the electrons would be released back to the conduction band of the MOS, leading to the increase of the conductivity of the sensing materials. An example of this conflict is given below.

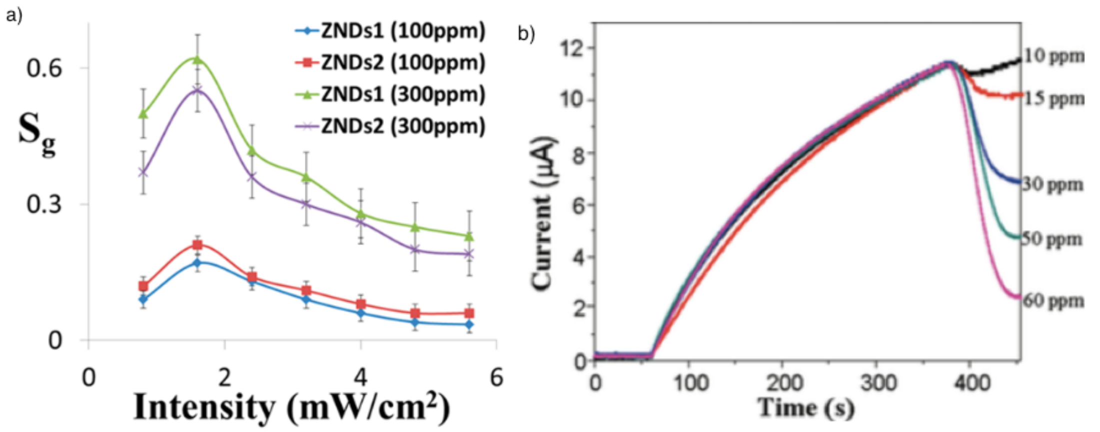

Figure 2.9 (a) Light intensity vs. sensitivity for 100 and 300 ppm of ethanol[36]; (b) current responses of the ZnO fiber sensor to ethanol gas with different ethanol concentrations[40]

The S_g in **Figure** 2.9 (a) is defined as $(I_g - I_a)/I_a$, where I_g is the sensor current value in the tested gas environment and I_a is the current value in air. Because S_g is positive, the current increased upon injection of ethanol. The chemical reactions given in this study are[36]:

$$CH_3CH_2OH + O^- \rightarrow C_2H_4O + H_2O + 1e^-$$

$$CH_3CH_2OH + O^{2-} \rightarrow C_2H_4O + H_2O + 2e^-$$

Those electrons are released back to the conduction band, therefore, the resistance decreases. In **Figure** 2.9 (b), the current decreased in the ethanol atmosphere. The typical reactions provided are[40]:

$$CH_3CH_2OH + 2h^+ \rightarrow CH_3CHO + 2H^+$$

$$CH_3CHO + 2O_2 + 2h^+ \rightarrow 2CO_2 \uparrow + H_2O + 2H^+$$

$$2H^+ + 2e^- \rightarrow H_2$$

Because the photochemical reactions consume both holes and excited electrons, the current of the sensor decreases. Although the two mechanisms given here can explain their own experimental results, they can elucidate each other. Therefore, the new theory should also be able to resolve this conflict, which has to be further verified by experimental results.

Chapter 3 Our New Hypothesis and Verification

3.1 Solving the conflict between the two redox processes

A typical current response of a MOS sensor to the UV exposure times is shown in **Figure 3.1 (a)**[40].

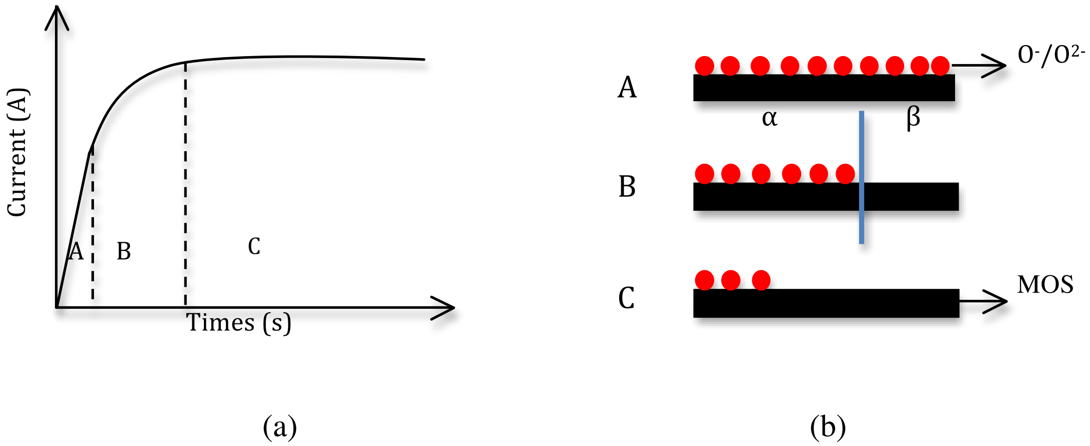

(a) (b)

Figure 3.1 (a) Schematic illustration of the current response of a MOS sensor to UV irradiation. (b) Schematic illustration of the adsorbed oxygen species on a sensor surface.

There are three regions in the current response curve: A is the fast-rise region, B is the slow-rise region and C is the constant region. The current rise in region A is attributed to the instant generation of electron-hole pairs upon excitation of UV light, which increases the carrier density. The slow rise in region B is due to the recombination reaction between the adsorbed oxygen species[36] and holes that migrate from bulk to surface. And region C is when the concentration of adsorbed oxygen reaches a dynamic equilibrium value. Correspondingly, the schematic concentrations of adsorbed oxygen species in three regions are shown in **Figure** 3.1(b). Because the carrier generation process takes place instantaneously, the desorption of oxygen species can be negligible in region A, where adsorption dominates. The beginning of desorption starts in region B, however. A gradual decrease of the oxygen concentration occurs until the stage of dynamic equilibrium concentration is reached. Two surface states can be assigned to the MOS surface as α and β. α is where the MOS surface is adsorbed with oxygen species and β is where no adsorption occurs. Once a RA is introduced, the reaction that takes place in region α is the chemical reaction between the RAs and adsorbed oxygen ion[36]. If we take ethanol as an example, the reactions involved are listed in equations below[36].

$$CH_3CH_2OH + O^-{}_{(ads)} \rightarrow C_2H_4O + H_2O + 1e^-$$

$$CH_3CH_2OH + O^{2-}{}_{(ads)} \rightarrow C_2H_4O + H_2O + 2e^-$$

The electrons will be released from oxygen ions and come back to the conduction band of MOS. So the conductivity or photocurrent will increase. This process can be defined as the carrier receiving process for the MOS. On the other hand, the reaction involved in region β is directly between the MOS and the RAs[41]. The typical reactions are as follows[40]:

$$CH_3CH_2OH + 2h^+ \rightarrow CH_3CHO + 2H^+$$

$$CH_3CHO + 2O_2 + 2h^+ \rightarrow 2CO_2 \uparrow + H_2O + 2H^+$$

$$2H^+ + 2e^- \rightarrow H_2$$

Because these reactions consume both holes and excited electrons, the conductivity or photocurrent decreases. And this process can be described as the carrier consuming process. The conflict between the two existing mechanisms found in literature can now be explained by the following model; if the reaction is dominated by α region, the overall current increase will be larger than the decrease. The final outcome that can be observed is the net current increase. And the current decrease can be shown when the β reaction or the carrier consuming reaction dominates. Since the adsorbed oxygen concentration can be altered by UV light intensity or exposure time, therefore the photocurrent can either be increased or decreased depending on the two processes.

3.2 Solving the selectivity problem

The optimum intensity for an analyte thus takes place at the point where the consumption of the carriers begins to exceed the reception of the carriers for the MOS. The selectivity mechanism can now be resolved by this model. Variable RAs react with the oxygen ions differently. The reducing ability of the analytes under UV light will affect the redox reaction thus influence the amount of oxygen ions desorbed by the analytes as described by equations 1 and 2, which will be further illustrated by **Figure** 3.2.

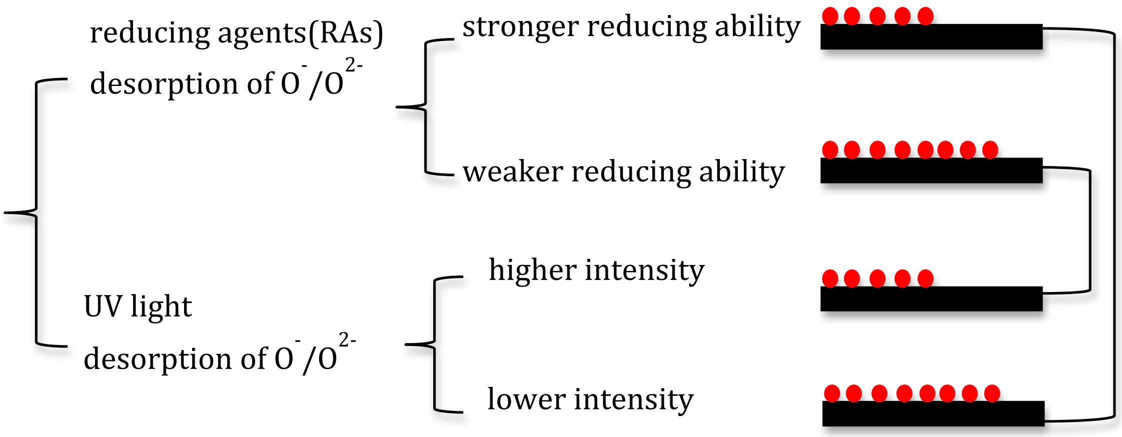

Figure 3.2 Schematic representation of the influences of UV light intensity and the analyte reducing ability under UV light on adsorbed oxygen species concentration.

A RA with stronger reducing ability under UV light can desorb more oxygen ions than a RA with weaker reducing ability. Thus the analyte with stronger reducing ability only needs a lower amount of UV light to reach the dynamic equilibrium concentration. And the analyte with weaker reducing ability will require stronger intensity to achieve the balance. So the differences in RAs' reducing abilities under UV light will produce variable optimum intensities. However, with changing analyte concentration the optimum intensity value remains the same, which may be attributed to the saturation of the analyte on the MOS surface. The amount of desorption of oxygen species will not change for different analyte concentrations, once the saturation stage is reached.

3.3 Experimental verification

Experiments were therefore designed to prove the proposed reaction mechanism by varying the adsorbed oxygen concentration on the MOS surface, and by observing the photocurrent change upon acetone injection. Annealing of the MOS sensors in oxygen atmosphere will give rise to chemisorbed oxygen[58] and long time UV light exposure can reduce the chemisorbed oxygen.

The experiment results are shown in **Figure** 3.3. Before annealing, little amount of oxygen species was adsorbed on the sensor surface, and the current decreased upon the injection of acetone. The decrease in background current after annealing is due to the scattering of free carriers by ionized impurities[59] and the increased amount of adsorbed oxygen. Sharp increases of the photocurrent can be observed after the injection of acetone. And after 24 hours of oxygen desorption by the UV light, the current dropped again. Thus a conclusion can be made, such that the variation in adsorbed oxygen concentration indeed changes the reaction mechanism between the carrier receiving and consuming types. Thus the experimental results support the proposed reaction mechanism for the UV-light activated MOS gas sensors.

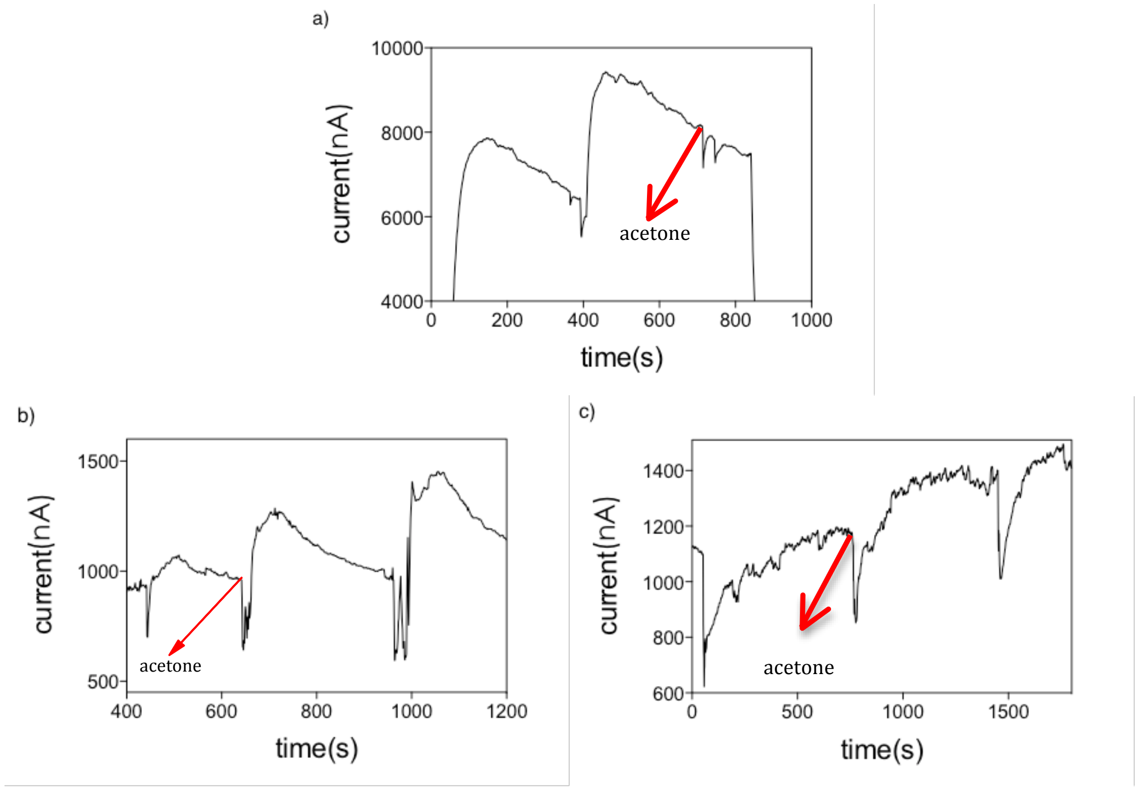

Figure 3.3**.** Current responses of the ZnO film sensor to acetone vapor under UV irradiation: (a) Current response before annealing. (b) Current response after annealing under 350°C for two hours. (c) Current response of the annealed sample after 24 hours of UV light treatment.

Chapter 4 Experimental Procedures

4.1 Sensor material, substrate and fabrication

Nanoparticles of zinc oxide (99.9%, APS 87 nm, specific surface area 15-25 m^2/g) were obtained from Aldrich Chemical Co. The substrate is shown in **Figure** 4.1. Two ITO stripes are placed on a glass substrate and connected to the electrodes of the testing system. The zinc oxide MOS material is placed on top of the two stripes and constitutes the electrical circuit.

The zinc oxide nanopowder was placed in an agate pestle and mortar and a certain amount of distilled water was added to form a thick slurry[35]. Then 3 mL of the zinc oxide paste was added on the substrate to from a thin film. The sample was dried in room temperature and atmosphere for 24 hours.

4.2 Sensor testing

The sensor performance was then tested by a Pico Ampere Meter (Keithley 485) as shown in **Figure** 4.1. The voltage applied to the sensor was 10 V.

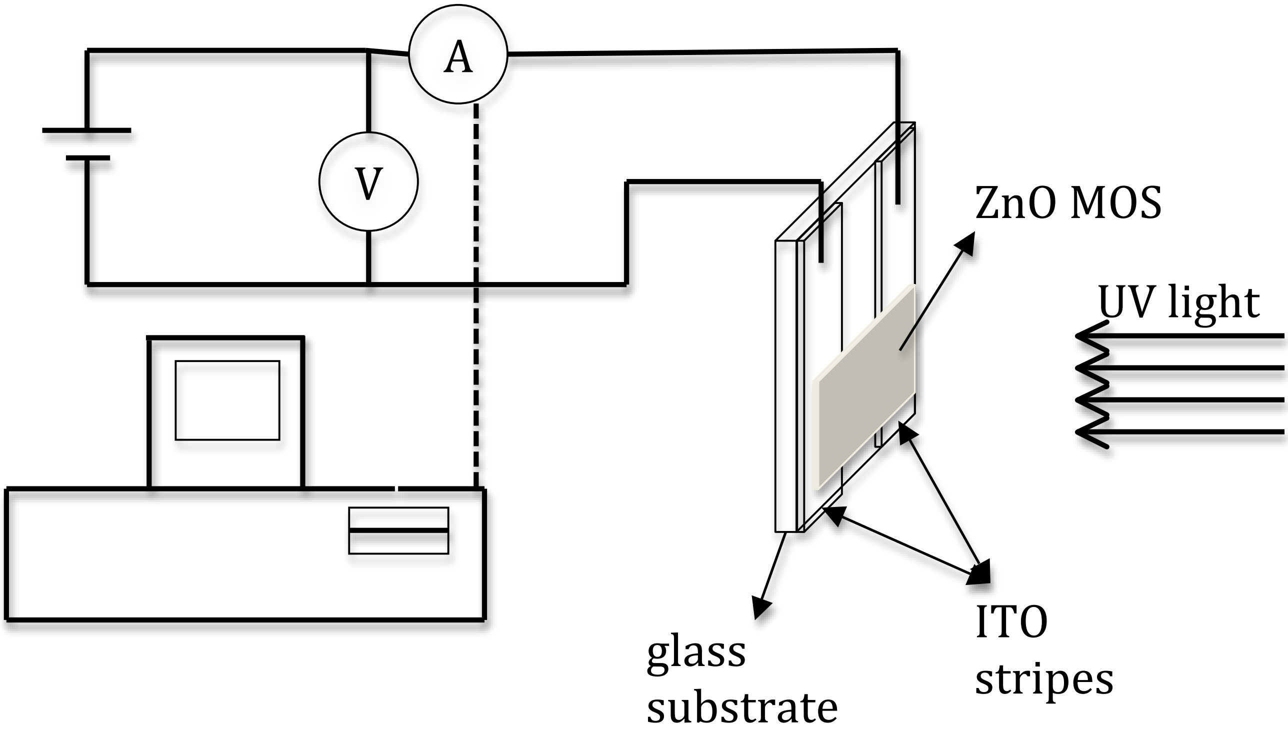

Figure 4.1 Schematic diagram of the sensor testing system

The back of the sensor was attached to a fixed point on a white board. A high intensity

UV lamp (B-100AP UV lamp, Co. UVP) that peaks at 365 nm was placed 15 inches away from the sample to provide an intensity about 3 mW/cm^2. The test gas was provided by a nitrogen tank containing 200 ppm acetone. The UV light was turned on for 5 minutes before the injection of the acetone to gain a relatively stable baseline. The same sample must be used for the three conditions: before annealing, after annealing and after 24h of UV light treatment.

Chapter 4 Conclusion

To summarize, a new reaction mechanism based on the concept of dynamic equilibrium concentration of adsorbed oxygen was proposed in this report to resolve the selectivity mechanism of the UV-light activated MOS gas sensor. The conflict between the two existing reaction mechanisms that have not been discussed together was accommodated by this new model as well. The optimum intensity was found at the point where the consumption of the carriers prevails the releasing of the carriers. All these have been approved experimentally by changing the amount of adsorbed oxygen species on the sensor surface, where the sensor performance is shown by the photocurrent increase or decrease.

Bibliography

[1] A. Tricoli, M. Righettoni, A. Teleki, “Semiconductor gas sensors: dry synthesis and application”, *Angewandte Chemie International Edition*, 2010, **49**, 7632.

[2] L. Pauling, A. B. Robinson, R. Teranishi, P. Cary, “Quantitative analysis of urine vapor and breath by gas-liquid partition chromatography”, *Proceedings of the National Academy of Sciences of the United States of America*, 1971, 68, 2374.

[3] W. Cao, Y. Duan, “Breath analysis: potential for clinical diagnosis and exposure assessment”, *Clinical chemistry,* 2006, **52**, 800.

[4] B. d. L. Costello, A. Amann, H. Al-Kateb, C. Flynn, W. Filipiak, T. Khalid, D. Osborne, N. M. Ratcliffe, “A review of the volatiles from the healthy human body”, *Journal of breath research*, 2014, **8**, 014001.

[5] T. Ligor, M. Ligor, A. Amann, C. Ager, M. Bachler, A. Dzien, B. Buszewski, “The analysis of healthy volunteers' exhaled breath by the use of solid-phase microextraction and GC-MS”, *Journal of breath research,* 2008, **2**, 046006.

[6] K. H. Kim, S. A. Jahan, E. Kabir, “A review of breath analysis for diagnosis of human health”, *TrAC Trends in Analytical Chemistry,* 2002, **109**, 615.

[7] P. Montuschi, P.J. Barnes, "Exhaled leukotrienes and prostaglandins in asthma", *J. Allergy. Clin. Immunol,* 2002, **109**, 615.

[8] M. I. Friedman, G. Preti, R.O. Deems, L. S. Friedman, S. J. Munoz, W. C. Maddrey , "Limonene in expired lung air of patients with liver disease", *Dig. Dis. Sci*, 1994, **39**, 1672.

[9] M. Phillips, R. N. Cataneo, B. A. Ditkoff, P. Fisher, J. Greenberg, R. Gunawardena, C.S. Kwon, O. Tietje, C. Wong, "Prediction of breast cancer using volatile biomarkers in the breath", *Breast Cancer Res. Treat*, 2006, **99**. 19.

[10] G. E. Carpagnano, S. A. Kharitonov, O. Resta, M. P. Foschino-Barbaro, E. Gramiccioni, P. J. Barnes, "Increased 8-Isoprostane and Interleukin-6 in Breath Condensate of Obstructive Sleep Apnea Patients" *Chest*, 2002, **122**, 1162.

[11] M. L. Simenhoff, J. F. Burke, J. J. Saukkonen, A. T. Ordinario, R. Doty, "Biochemical Profile of Uremic Breath", *N. Engl. J. Med*, 1977, **297**, 132.

[12] W. Chuji, A. Mbi, M. Shepherd, "A Study on Breath Acetone in Diabetic Patients Using a Cavity Ringdown Breath Analyzer: Exploring Correlations of Breath Acetone With Blood Glucose and Glycohemoglobin A1C", *Sensors Journal, IEEE*, 2010, **10**, 54.

[13] Wikipedia - Gas detector.

https://en.wikipedia.org/wiki/Gas_detector

[14] Wikipedia - Electrochemical gas sensor.

https://en.wikipedia.org/wiki/Electrochemical_gas_sensor

[15] J. Chou, "Hazardous Gas Monitors: A Practival Guide to Selection, Operation, and Applications - Chapter 2", *Mcgraw-Hill Book Company, New York,* 1999.

[16]http://www.envirotech-online.com/news/gas-detection/8/alphasense/low_ppb_detection_level_sensors/21887/

[17] Wikipedia - Catalytic bead sensor.

https://en.wikipedia.org/wiki/Catalytic_bead_sensor

[18] Operating principle - Catalytic-type gas sensor.

http://www.figaro.co.jp/en/technicalinfo/principle/catalytic-type.html

[19] Catalytic sensors.

http://www.sensitron.it/wp-content/uploads/2010/07/CatalyticSensors.pdf

[20] History of IR Gas Sensing.

http://www.edinburghsensors.com/Technology/history-of-ir-gas-sensing/

[21] Enggcyclopedia - How infrared gas detectors work.

http://www.enggcyclopedia.com/2011/11/infrared-gas-detectors/

[22] J. Chou, "Hazardous Gas Monitors: A Practival Guide to Selection, Operation, and Applications - Chapter 5", *Mcgraw-Hill Book Company, New York,* 1999.

[23] Key features of IR Gas Sensors.

http://www.edinburghsensors.com/Technology/key-features-ir-gas-sensors/

[24] Single vs Dual Wavelength Sensors.

http://www.edinburghsensors.com/Technology/single-vs-dual-wavelength-sensors/

[25] G. F. Fine, L. M. Cavanagh, A. Afonja, R. binions, "Metal oxide semi-conductor gas sensors in environmental monitoring", *Sensors*, 2010, **10**, 5469.

[26] C. X. Wang, L. W. Yin, L. Y. Zhang, D. Xiang, R. Gao, "Metal oxide gas sensors: Sensitivity and influencing factors", *Sensors*, 2010, **10**, 2088.

[27] X. Liu, S. Cheng, H. Liu, S. Hu, D. Q. Zhang, H. S. Ning, "A survey on gas sensing technology", *Sensors*, 2012, **12**, 9635.

[28] Operating principle - MOS-type gas sensor.

http://www.figaro.co.jp/en/technicalinfo/principle/mos-type.html

[29] The pros and cons of electrochemical sensors.

http://www.safetyandhealthmagazine.com/articles/the-pros-and-cons-of-electrochemical-sensors-2

[30] Combustible Gas Safety Monitoring: Infrared vs. Catalytic Gas Detectors.

http://www.gmigasandflame.com/downloads/white-papers/IR-vs-CatalyticBead-WhitePaper.pdf

[31] Electronic gas sensors and detectors - classification and operating principles.

http://www.electronics-base.com/general-description/gas-sensors/171-electronic-gas-sensors-and-detectors-clasification-and-operating-principles

[32] S. W. Fan, A. K. Srivastava, V. P. Dravid, "Nanopatterned polycrystalline ZnO for room temperature gas sensing", *Sensors and Actuators B,* 2010, **144**, 159.

[33] J. Herran, O. F. Gonzalez, I. C. Hurtado, T. Romero, G. G. Mandayo, E. Castano, "Photoactivated solid-state gas sensor for carbon dioxide detection at room temperature", *Sensors and Actuators B,* 2010, **149**, 368.

[34] J. Saura, "Gas-sensing properties of SnO_2 pyrolytic films subjected to ultrviolet radiation", 1994, **17**, 211.

[35] B. P. J. de Lacy Costello, R. J. Ewen, N. M. Ratcliffe, M. Richards, "Highly sensitive room temperature sensors based on the UV-LED activation of zinc oxide nanoparticles", *Sensors and Actuators B,* 2008, **134**, 945.

[36] M. R. Alenezi, A. S. Alshammari, K. D. G. I. Jayawardena, M. J. Beliatis, S. J. Henley, S. R. P. Silva, "Role of the Exposed Polar Facets in the Performance of Thermally and UV Activated ZnO Nanostructured Gas Sensors", *The Journal of Physical Chemistry C,* 2013, **117**, 17850.

[37] S. Mishra, C. Ghanshyam, N. Ram, R.P. Bajpai, R. K. Bedi, "Detection mechanism of metal oxide gas sensor under UV radiation", *Sensors and Actuators B*, 2004, **97**, 387.

[38] X. D. Wang, S. S. Yee, W. P. Carey, “Transition between neck-controlled and grain-boundary-controlled sensitivity of metal-oxide gas sensors”, *Sensors and Actuators B,* 1995, **24**, 454.

[39] J. D. Prades, R. J. Diaz, M. Manzanares, F. H. Ramirez, A. Cirera, A. R. Rodriguez, S. Mathur, J. R. Morante, “A model for the response towards oxidizing gases of photoactivated sensors based on individual SnO_2 nanowires”, *Physical Chemistry Chemical Physics,* 2009, **11**, 10881.

[40] J. Gong, Y. H. Li, X. S. Chai, Z. S. Hu, Y. L. Deng, “UV-light activated ZnO fibers for organic gas sensing at room temperature”, *The Journal of Physical Chemistry C,* 2010, **114**, 1293.

[41] Y. H. Li, J. Gong, G. H. He, Y. L. Deng, “Enhancement of photoresponse and UV-assisted gas sensing with Au decorated ZnO nanofibers”, *Materials Chemistry and Physics*, 2012, **134**, 1172.

[42] S. W. Fan, A. K. Srivastava, V. P. Dravid, “Nanopatterned polycrystalline ZnO for room temperature gas sensing”, *Sensors and Actuators B,* 2010, **144**, 159.

[43] Y. Zhang, B. K. Liu, D. J. Wang, Y. H. Lin, T. F. Xie, J. L. Zhai, “Photoelectric properties of ZnO/Ag_2S heterostructure and its photoelectric ethanol sensing characteristics”, *Materials Chemistry and Physics,* 2012, **133**, 834.

[44] N. Barsan, M. S. Berberich, W. Gopel, “Fundamental and practical aspects in the design of nanoscaled SnO_2 gas sensors: a status report”, *Fresenius' Journal of Analytical Chemistry*, 1999, **365**, 287.

[45] L. Kronik, Y. Shapira, “Surface photovoltage spectroscopy of semiconductor structures: at the crossroads of physics, chemistry and electrical engineering”, *Surface and Interface Analysis*, 2001, **31**, 954.

[46] J. D. Prades, F. H. Ramirez, R. J. Diaz, M. Manzanares, T. Andreu, A. Cirera, A. R. Rodrigues, J. R. Morante, “The effects of electron-hole separation on the photoconductivity of individual metal oxide nanowires”, *Nanotechnology*, 2008, **19**, 465501.

[47] E. Comini, L. Ottini, G. Faglia, G. Sberveglieri, “SnO_2 RGTO UV activation for CO monitoring”, *IEEE Sensors Journal,* 2004, **4**, 17.

[48] A. Ponzoni, E. Comini, I. Concina, M. Ferroni, M. Falasconi, E. Gobbi, V. Sberveglieri, G. Sberveglieri, “Nanostructured metal oxide gas sensors, a survey of applications carried out at SENSOR lab, Brescia (Italy) in the security and food quality fields”, *Sensors*, 2012, **12**, 17023.

[49] G. Korotcenkov, “Metal oxides for solid-state gas sensors: What determines our choice?”, *Materials Science and Engineering B*, 2007, **139**, 1.

[50] N. Barsan, U. Weimar, “Conduction model of metal oxides gas sensors”, *Journal of Electroceramics,* 2001, **7**, 143.

[51] S. Choopun, N. Hongsith, E. Wongrat, Metal-Oxide Nanowires for Gas Sensors. http://dx.doi.org/10.5772/54385

[52] Wikipedia - Electronic band structure. https://en.wikipedia.org/wiki/Electronic_band_structure

[53] Chemwiki - Band Theory of Semiconductors. http://chemwiki.ucdavis.edu/u_Materials/Electronic_Properties/Band_Theory_of_Semiconductors

[54] Wikipedia - Valence and conduction bands. https://en.wikipedia.org/wiki/Valence_and_conduction_bands

[55] S. W. Fan, A. K. Srivastava, V. P. Dravid, "UV-activated room-temperature gas sensing mechanism of polycrystalline ZnO", *Applied Physics Letters,* 2009, **95**, 142106.

[56] N. Takubo, Y. Muraoka, Z. Hiroi, "Conductivity switching by ultraviolet light in tin dioxide thin films", *Applied Physics Express,* 2009, **2**, 045501.

[57] P. Feng, X. Y. Xue, Y. G. Liu, T. H. Wang, "Highly sensitive ethanol sensors based on {100}-bounded In_2O_3 nanocrystals due to face contact", *Applied Physics Letters,* 2006, **89**, 243514.